

## MODULAR FRP SANDWICH ASSEMBLIES FOR ONE-WAY AND TWO-WAY SLAB AND COMPOSITE BEAM APPLICATIONS

Yu Bai<sup>1</sup> and Sindu Satasivam<sup>2</sup>

<sup>1</sup>Professor, Department of Civil Engineering, Monash University, Clayton, Melbourne, Australia. Tel: ++61 3 9905 4987; Fax: +61 3 9905 4944; Email: yu.bai@monash.edu

<sup>2</sup>Former research fellow in the Department of Civil Engineering, Monash University; currently Structural Engineer at Lendlease Australia; Email: s.satasivam@gmail.com

### 1. INTRODUCTION

Fibre reinforced polymer (FRP) composite materials have become as primary load-carrying structural members in civil construction [1]. They provide high strength, come in a variety of colours and transparencies and are lightweight, chemically unreactive and resistant to corrosion [2]. FRP composites, particularly if glass fibres are used (i.e. glass fibre reinforced polymers, or GFRP), also exhibit low thermal conductivity and embodied energy. However, in comparison to steel, GFRP materials are associated with a low material stiffness resulting from a low elastic modulus (10-20% that of steel). This makes the deflection criteria in serviceability limit state (SLS) design of GFRP structures even more critical than strength design. GFRP is a linear-elastic material, resulting in sudden and brittle failures. The fibre architecture of GFRP materials also bring stiffness of the longitudinal direction (also known as the pultrusion direction, in which the majority of the fibres run) much larger than that in the transverse direction.

A modular sandwich design concept is developed to consider such specific material features for building construction, where built-up beam or slab sections consisting of pultruded GFRP box or I-profiles are sandwiched between GFRP flat panels to form a web-flange structure. This section has an improved second moment of area, thereby improving the stiffness of GFRP at the structural level. The use of pre-fabricated built-up profiles provides greater flexibility in designing floor systems, which may be advantageous than pultruded FRP decks with constant sections for varying load conditions. This design flexibility can also allow for the incorporation of two different pultrusion orientations into the one structure, which may improve strength in transverse direction and avoid premature cracking in this direction. In addition, by using built-up GFRP members, pre-fabricated foam blocks can be easily incorporated during fabrication of the modular assembly to further enhance structural performance. Finally, the inclusion of steel as a supporting girder to form composite beams may provide ductile responses if properly designed.

The paper summarizes the investigations on the mechanical performance under static loading for such modular GFRP sandwich structures in applications of one-way spanning slabs (or beams), two-way spanning slabs and GFRP-steel composite beams [3-6]. The bending stiffness, load-carrying capacity, failure mechanism and composite action were evaluated and analyzed. In addition, two different pultrusion configurations were achieved and examined in the two-way slabs and GFRP-steel composite beams: flat panels with pultrusion directions either parallel or perpendicular to the web-core profiles. The latter can effectively avoid premature cracking along the pultrusion direction of the face flat panels. Furthermore, the GFRP-steel composite beams were appropriately designed since they showed ductile load-deflection responses that resulted from yielding of the steel girder, which commenced prior to failure of the GFRP slabs.

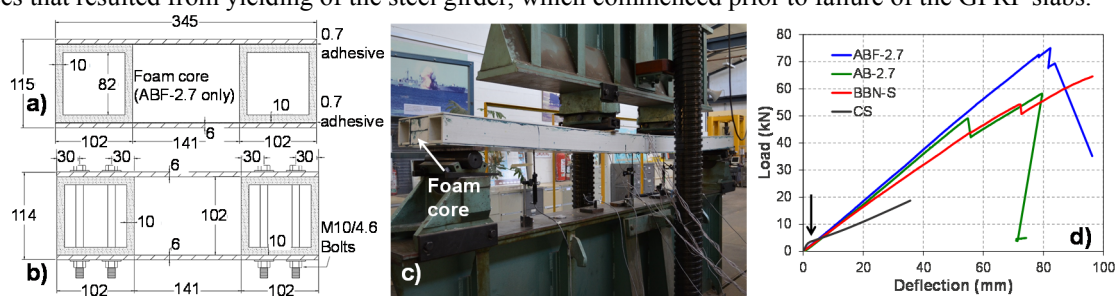


**Fig. 1: Modular FRP sandwich beams (a) sections for AB-2.7 and ABF-2.7; (b) section for BBN-2.7; (c) specimen ABF-2.7 under bending and (d) load displacement curves for all specimens compared with a designed reinforced concrete one way slab.**

### 2. ONE-WAY BENDING APPLICATIONS

Three modular sandwich beams (AB-2.7, ABF-2.7 and BBN-2.7) were fabricated from pultruded GFRP materials (box sections and flat panels as shown in Fig. 1(a) and (b)), consisted of E-glass fibres and polyester resin with volume fraction of 42-48% and 53-58% respectively. The material properties of the GFRP materials were determined as 306 MPa for tensile strength, 30 GPa for Tensile modulus, and 27 MPa for the interlaminar shear strength. Araldite 420 epoxy adhesive with a 25 MPa shear strength was utilized for the bonding. Divinycell P150 Foam, supplied by DIAB Australia, was utilized as a core material (only for ABF-2.7 see Fig. 1(c)). Zinc-plated M8 and M10 steel bolts were used for

preparation of specimen BBN-2.7 (Fig. 1(b)). The bolts were class 4.6 with a bolt diameter of 8mm (M8) or 10 mm (M10), a nominal tensile strength of 400 MPa and a proof load stress of 225 MPa.

All specimens (both adhesively bonded and bolted) had lengths of 2.7m (therefore with span-to-depth ratios about 25) and widths of 345mm. For specimens AB-2.7 and ABF2.7 with adhesive bonding, a layer of Araldite epoxy adhesive with a thickness of 0.7mm was used to adhesively bond the GFRP components and foam components. M10 bolts were used in a staggered configuration to connect the flat panels to the box profiles at a spacing of 150mm for specimen BBN-2.7. All specimens were simply supported and loaded in four-point bending, with the distance of 900mm between the point loads and the supports. Loading was applied as a displacement control mode of 3.5mm/min.

The load  $P_1$ , in which material failure of the upper panel (rather than structural ultimate failure) arose due to local buckling, occurred in specimen ABF-2.7 at 73kN (see Fig. 1(d)). A smaller  $P_1$  load seen in AB-2.7 is because the upper panel of AB-2.7 was bonded only to the box profiles; whereas the whole upper panel of ABF-2.7 was restrained as it was bonded to both the box-profiles and the foam core. Furthermore the presence of foam in this study represents an increase in weight of only 15%, the addition of such lightweight materials can improve the load-carrying capacity of GFRP sandwich structures. Both adhesively bonded specimens AB-2.7 and ABF2.7 demonstrated a higher bending stiffness than that of the bolted specimen BBN-2.7 especially at later loading stages as shown in Fig. 1(d), due to a partial composite action. All specimens finally failed at the web flange junction followed by the web buckling.

A RC member, designated CS, was designed according to AS3600 with the same cross-section dimensions ( $345 \times 115$ mm reinforced by six N10 tensile bars and four N10 compressive bars) and same span length (2.7m) as those of the GFRP sandwich specimens. Under four-point bending, the failure load of CS was calculated to be 20kN per point load, which is equivalent to an ultimate moment capacity of 18kNm. The cracking moment of the concrete slab was calculated as 2.8kNm, corresponding to a load of 3kN under four-point bending. After the cracking moment, deflections were calculated based on the effective second moment of area of the cracked section. The load-deflection curve of CS is provided in Fig. 1(d) for comparison.

It can be seen that GFRP sandwich specimens showed favourable properties compared to the one-way spanning RC slab of the same sectional size. The sandwich specimens AB-2.7 and ABF-2.7 were about 80% lighter than CS (which weighed 100 kg/m), but their ultimate loads were about 2 to 2.5 times greater than that of CS. Prior to cracking, the bending stiffness of CS was  $13.9 \times 10^{11}$  Nmm<sup>2</sup>, larger than that of sandwich specimens AB-2.7 and ABF-2.7 (at  $6.2 \times 10^{11}$  Nmm<sup>2</sup> and  $6.9 \times 10^{11}$  Nmm<sup>2</sup> respectively). However, once cracking occurred for CS, its effective section and therefore stiffness was greatly reduced as shown in Fig. 1(d). The SLS is reached in this post-cracking stage, where the effective bending stiffness of the cross-section is  $5.2 \times 10^{11}$  Nmm<sup>2</sup>, up to 25% less than the stiffness of the GFRP specimens.

### 3. TWO-WAY BENDING APPLICATIONS

Four modular GFRP sandwich two-way spanning slabs were fabricated and tested. Each specimen was made from seven  $50 \times 50 \times 6$  mm GFRP box profiles sandwiched between 6 mm-thick flat GFRP panels. Each sandwich slab had a total depth of 62 mm, an overall length and width of  $1.5 \times 1.5$  m, a span of  $1.45 \times 1.45$  m, and was supported on all four sides by steel rollers. Three sandwich slabs (UA, BA and BAF) had an adhesively bonded connection. Sandwich slab UA had a unidirectional pultrusion orientation where the pultrusion direction of the upper and lower flat panels lay parallel to the pultrusion direction of the box profiles (Fig. 2(a)). Sandwich slabs BA, BAF and BB all had bidirectional pultrusion orientations, where the pultrusion direction of the upper and lower flat panels lay in the transverse slab direction, perpendicular to that of the box profiles (Fig. 2(b)). In addition, BAF also had six prefabricated foam blocks as the core of the structure between each box profile (see Fig. 2(b)). These foam blocks were adhesively bonded to the inner surfaces of the specimen. Finally, sandwich slab BB was fabricated by connecting the GFRP components with blind bolts at a practical spacing of 150 mm along the longitudinal slab direction to achieve partial shear interaction.

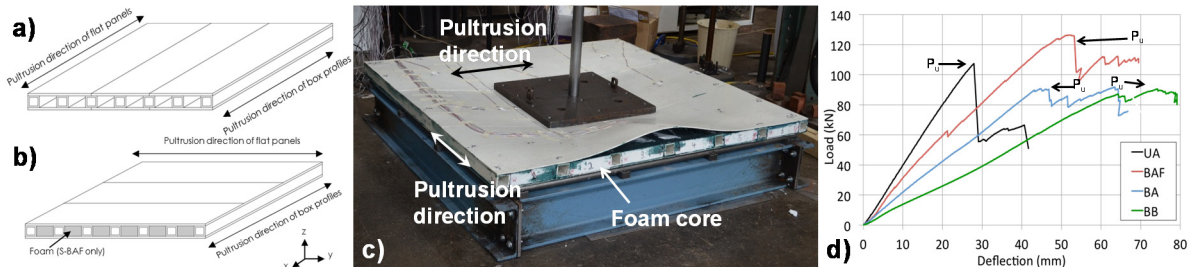


**Fig. 2: Modular GFRP sandwich slabs (a) and (b) specimen configurations; (c) specimen BAF at failure and (d) load displacement curves for all specimens.**

Load was applied at the central region of the slabs through a steel plate. The resulting bending caused cracking along the pultrusion direction between the fibres within the flat panel for the unidirectional sandwich slab UA at 65 kN. This longitudinal crack continued to elongate as loading increased. Slab UA failed at the ultimate load  $P_u$  of 107 kN, with the final failure occurred via in-plane shearing of box profiles. No premature local cracking was observed in the bidirectional

slabs BA, BAF and BB. Instead, local out-of-plane buckling arose at the edges of those slabs as shown in Fig. 2(c). This local buckling continued to increase, causing the failure of the connection between the upper panel and the central box profile. Such progressive failures developed in the connection region until in-plane shear failure of box profiles occurred at the ultimate loads of 90 kN for specimen BA, of 126 kN for BAF, of 88 kN for BB.

As shown in Fig. 2(d), the sandwich slab with the greatest stiffness was UA (unidirectional pultrusion orientation and adhesive bonding). When the pultrusion direction of the flat panel was placed perpendicular to that of the box profiles, the bending stiffness was reduced obviously as in BA. The stiffness of the slab BAF, with the foam core and adhesive bonding, was 45% greater than that of BA and 20% less than that of UA. The addition of foam provided a significant increase in stiffness, even though the foam core was associated with a low elastic modulus of 115 MPa (corresponding to only 0.4% of that of the GFRP box profiles). The slab with the lowest stiffness was BB, in which the stiffness was 40% less than that of BA, because of bolted connections provided partial composite action in comparison to the full composite action offered by the adhesive bonding.

#### 4. COMPOSITE BEAM APPLICATIONS

Four GFRP-steel composite beams (UA, BA, UB and BB) were fabricated, with the first letter refers to the pultrusion configuration of the sandwich slab (U=unidirectional, B=bidirectional) and the second letter refers to the connection type between the slab and the steel beam (A=adhesive, B=bolted). A reference steel beam was also tested.

The overall length of each specimen was 3 m, and the span length was 2730 mm. The depth of each sandwich slab was 62 mm, and they were connected to steel beams with a depth of 155 mm, giving an overall composite beam depth of 217 mm. The width of each FRP slab was 500 mm. Fig. 1(a) shows the side view for the bidirectional beams BA and BB (bolts between the slab and steel beam used only for BB and UB); and Fig. 1(b) shows that for UA and UB.

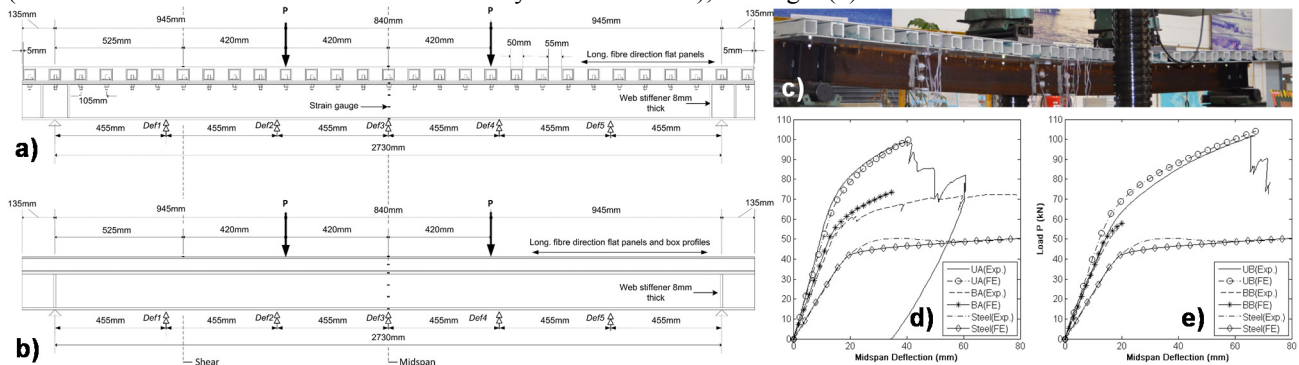


**Fig. 3: Modular GFRP-steel composite beams (a) specimen BB and (b) UA in side view; (c) deformed shape of specimen BB with yielding of steel girder; (d) and (e) load displacement curves for all specimens.**

Composite beam BA experienced local crushing of a box profile situated directly beneath a loading point at a load of 53 kN. Further increase in load until 72 kN was associated with a large increase in deformation due to the yielding of steel girder (Fig. 3(d)). This load (72kN) was recorded as its maximum load (Pmax), and was 40% higher than the maximum load of the reference steel beam (52 kN). Composite beam BB presented a maximum load of 79 kN (not recorded in Fig. 3(e)) and failed via in-plane shearing of the GFRP slab and then the experiment was manually stopped because of excessive large bending deformation (Fig. 3(c)). The local crushing of box profiles beneath the point load that was observed in BA was avoided in BB by the use of a greater steel plate width of 200 mm. The maximum failure load of unidirectional composite beam UA and UB was reached at 99 kN and 102 kN respectively, when the beams failed via longitudinal shear of the upper and lower panels. Again such failures of FRP sandwich slabs occurred after the excessive yielding of the supporting steel girders.

#### ACKNOWLEDGEMENTS

The authors thank the supports from the Australian Research Council through DE120101913 and DP180102208.

#### REFERENCES

- [1] L.C. Bank, *Composites for construction: structural design with FRP materials*. John Wiley & Sons, Inc., 2007.
- [2] T. Keller, C. Haas and T. Vallée. “Structural concept, design and experimental verification of a GFRP sandwich roof structure”, *Journal of Composites for Construction*, 2008; 12/4: 454-468.
- [3] S. Satasivam, Y. Bai, X.L. Zhao. Adhesively bonded modular GFRP web-flange sandwich for building floor construction. *Composite Structures*, 2014; 111: 381-392.
- [4] S. Satasivam, Y. Bai. Mechanical performance of bolted modular GFRP composite sandwich structures using standard and blind bolts. *Composite Structures*, 2014; 117: 59-70.
- [5] S. Satasivam, Y. Bai, Y. Yang, L. Zhu, X.L. Zhao. Mechanical performance of two-way modular FRP sandwich slabs. *Composite Structures*, 2018; 184: 904-916.
- [6] S. Satasivam, Y. Bai. Mechanical performance of modular FRP-steel composite beams for building construction. *Materials and Structures*, 2016; 49(10): 4113-4129.